

Surface Water Stable Isotope Geochemistry in King George Island, Antarctica

Aurel Persoiu¹, Carmen-Andreea Bădăluță², and Jeonghoon Lee³

¹Emil Racoviță Institute of Speleology

²Ștefan cel Mare University

³Ewha Womans University

December 17, 2022

Abstract

The region around the tip of the Antarctic Peninsula is one of the fastest warming regions of the world, a situation that will lead to widespread changes in permafrost state, local hydrological cycles and biological activity. Further, it is located in the path of the southern westerly winds, one of the poorest-understood components of the global climatic system. The sedimentary archives in the lakes from the ice-free regions on this region host a yet untapped wealth of information on the past changes and links between the regional climatic, hydrologic and biological systems. Especially important are the stable isotope compositions of these sediments, but to understand how they record these changes, an in-depth knowledge of their links to present-day conditions is required. We present here the first study of the stable isotope composition of the surface waters in the ice-free southern peninsulas of King George Island, Antarctica. Our results suggest that a clear separation of the various water bodies (permafrost, snow, meltwater, lakes) based on the stable isotope composition of the water is possible, allowing for future studies aiming to understand (changing) feeding behavior of terrestrial fauna. Further, water in lakes on a W-E transect have distinct stable isotope composition, leading to the possibility of studying the past changes in the strength and dynamics of the westerly winds in the region.

Hosted file

952092_0_art_file_10535007_rmvj7y.docx available at <https://authorea.com/users/567096/articles/613606-surface-water-stable-isotope-geochemistry-in-king-george-island-antarctica>

Surface Water Stable Isotope Geochemistry in King George Island, Antarctica

Aurel Perşoiu^{1,2}, Carmen-Andreea Bădăluță², and Jeonghoon Lee³

¹Emil Racoviță Institute of Speleology, Romanian Academy, Cluj-Napoca, Romania.

²Stable Isotope Laboratory, Ștefan cel Mare University, Suceava, Romania.

³Department of Science Education, Ewha Womans University, Seoul, Republic of Korea.

Corresponding author: Aurel Perşoiu (aurel.persoiu@gmail.com, aurel.persoiu@usv.ro)

Key Points:

- Clear separation of water bodies in terms of stable isotope composition
- General tendency towards lower $\delta^{18}\text{O}$ and $\delta^2\text{H}$ values with increased distance from the Bellingshausen Sea in the lake waters
- Possible step towards reconstructions of wind directions in the Southern Hemisphere westerly wind belt

44 Abstract

45 The region around the tip of the Antarctic Peninsula is one of the fastest warming regions of the
46 world, a situation that will lead to widespread changes in permafrost state, local hydrological
47 cycles and biological activity. Further, it is located in the path of the southern westerly winds,
48 one of the poorest-understood components of the global climatic system. The sedimentary
49 archives in the lakes from the ice-free regions on this region host a yet untapped wealth of
50 information on the past changes and links between the regional climatic, hydrologic and
51 biological systems. Especially important are the stable isotope compositions of these sediments,
52 but to understand how they record these changes, an in-depth knowledge of their links to present-
53 day conditions is required. We present here the first study of the stable isotope composition of
54 the surface waters in the ice-free southern peninsulas of King George Island, Antarctica. Our
55 results suggest that a clear separation of the various water bodies (permafrost, snow, meltwater,
56 lakes) based on the stable isotope composition of the water is possible, allowing for future
57 studies aiming to understand (changing) feeding behavior of terrestrial fauna. Further, water in
58 lakes on a W-E transect have distinct stable isotope composition, leading to the possibility of
59 studying the past changes in the strength and dynamics of the westerly winds in the region.
60

61 1 Introduction

62 Polar regions are experiencing rapid alterations of their hydrological cycles, linked to
63 accelerated warming over the past decades (Pacahuri et al., 2014; Walvoord & Kurylik, 2016),
64 alterations that are also affecting the structure, dynamics and functioning of local ecosystems
65 (Hass et al., 2010; Amesbury et al., 2018; Aracena et al., 2018). General climate warming will
66 result in complex changes of local climate components (e.g., Vaughan et al., 2003; Rückamp
67 et al., 2011; Turner et al., 2016), with their impact on local ecohydrology being difficult to assess in
68 the absence of baseline data (Gibson et al., 2015; Arnoux et al., 2017; Ala-aho et al., 2018) on
69 climate-hydrology-ecosystems links.

70 The majority of studies of the hydrological cycle in polar areas have focused on the
71 northern high-latitudes (Welp et al., 2005; Zacharavova et al., 2009; Delaveau et al., 2015;
72 Tetzlaff et al., 2018); with only few (Noon et al., 2002; Wand et al., 2011; Falk & Sala, 2015;
73 Gómez et al., 2017; Sziło & Bialik, 2017; Falk et al., 2018; Stowe et al., 2018) addressing related
74 issues in the Antarctic region. The massive Antarctic Ice Sheet leaves little land exposed at the
75 interface with the Southern Ocean. Such permanent ice-free areas are located on the edges of the
76 Antarctic Peninsula and the surrounding islands, a region that has had a strongly amplified and
77 complex response to the ongoing global warming. The region experienced one of the strongest
78 ($+0.32 \pm 0.2$ °C/decade) warming rates globally at the end of the 20th century (Turner et al., 2005),
79 followed by an even stronger ($-0.47 \sim -0.25$ °C/decade) cooling since about 1998 (Turner et al.,
80 2016). At the northern tip of the Antarctic Peninsula, King George Island (KGI, Figure 1) has a
81 series of ice-free peninsulas, hosting a complex network of linked lakes and rivers, fed by
82 glaciers, snow and rain, and underlain by a thick permafrost (Headland, 1984; Vieira et al., 2010;
83 Meredith et al., 2018). The seasonal melting of glaciers, snow cover and permafrost determines a
84 specific hydrology, with ephemeral streams linking permanent and temporary lakes, creating an
85 extensive network of wetlands. In permafrost areas, both short and long-term climatic changes
86 are affecting the depth of the active layer, affecting the hydrological connectivity (Quinton et al.,
87 2011), possibly leading to altered flow paths and increased discharge to inland lakes and the
88 open ocean (e.g., Peterson et al., 2002). Further, relative contribution of the different water

89 sources (precipitation, ice melt, snowmelt and groundwater) to surface flow changes on time
90 scales ranging from hours to decades (e.g., Barnett et al., 2005; Yde et al., 2016) and
91 understanding their dynamics on these time scales could lead to improved predictive skills for
92 hydrological models.

93 In studying the interactions between climate and the hydrological cycle, the stable
94 isotopes of hydrogen and oxygen are particularly useful, as they can track the origin of
95 precipitation, the variable contribution of various water sources (precipitation, snow, glacier and
96 permafrost melt) and the fluxes between the various water bodies (e.g., Gibson, 2005; Bowen,
97 2010; Wassenaar et al., 2011). The covariance between the ratios of heavy to light oxygen and
98 hydrogen isotopes in precipitation results in the possibility to construct Local Meteoric Water
99 Lines (LMWL, Craig, 1961) that can be used as a benchmark against which the same isotopic
100 ratios in lake, river, snow and permafrost water can be plotted and further analyzed in order to
101 disentangle hydrological sources, processes and mechanisms (e.g., Wassenaar et al., 2011).
102 Further, KGI is ideally located in the path of southern westerly winds, whose dynamics during
103 the Holocene (and beyond) has been the focus of intense scrutiny (Noon et al., 2003). Lack of
104 suitable paleorecords limits our understanding of the spatial and temporal dynamics of these
105 wind systems, and stable isotopes in lake sediments are one of the best proxies of such changes.
106 Studies in Maritime Antarctica (Noon et al., 2003) have shown that $\delta^{18}\text{O}$ values of lake
107 carbonates reflect changes in $\delta^{18}\text{O}$ of lake waters, in turn affected by climatic factors. However,
108 such studies are sparse in Maritime Antarctica, and a network of palaeoclimate reconstructions
109 are needed to better understand the spatial variability of past climate changes. Further,
110 calibration of climate proxies is needed and a first step in this approach is to understand the links
111 between climate and the stable isotope composition of lake waters. Lakes in KGI have been
112 shown to contain sediments rich in carbonates covering at least Holocene (Mäusbacher et al.,
113 1989; Hernández et al., 2018) thus offering the possibility to reconstruct the dynamics of
114 sedimentation and past climate variability, provided that we understand what the proxies in these
115 sediments record in terms of climate elements.

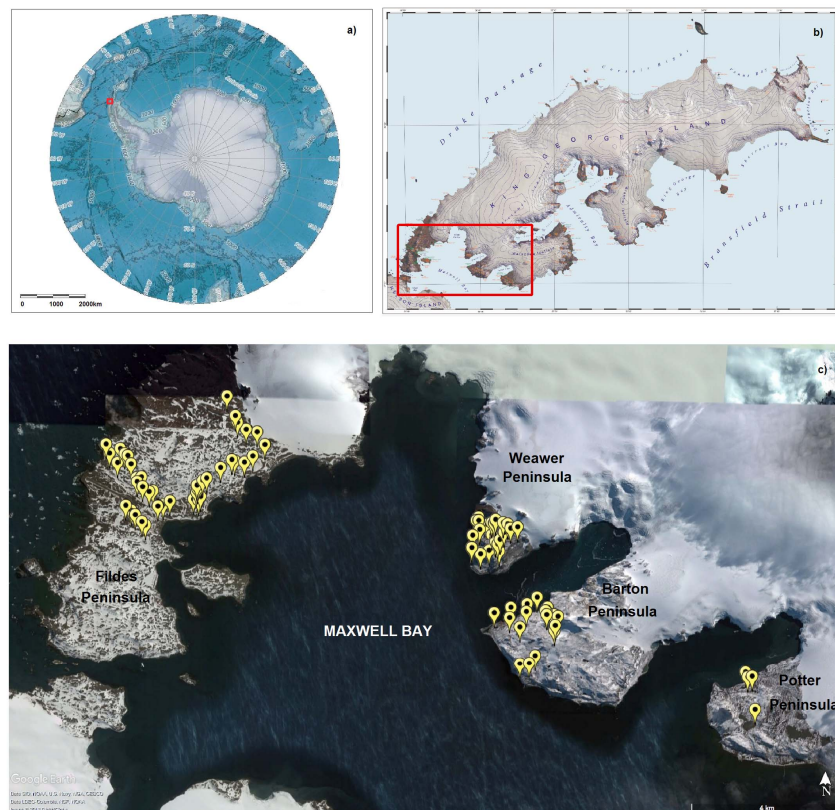
116 Here we present a first study of the isotopic composition of surface waters in the southern
117 peninsulas (Barton, Fildes, Weaver and Potter) of King George Island, Antarctica. The objectives
118 of our study were to 1) investigate the spatial distribution of oxygen and hydrogen stable
119 isotopes in lake waters, as a first step towards developing new proxies of past climate changes in
120 the areas and 2) disentangle the various water sources and reservoirs implicated in the summer
121 hydrological cycle.

122 **2 Data and methods**

123 2.1 Site description

124 King George Island is the largest landmass (1250 km²) of the South Shetland Islands,
125 lying about 120 km north of the West Antarctic peninsula (Figure 1a). A glacier cap covers 92 %
126 of the island, with only a few peninsulas (mainly in the SW) being ice-free (Figure 1b and 1c).
127 Two icefields (Arctowsky and Warszawa) form the northern boundary of the ice-free zones of
128 the four largest peninsulas: Fildes, Weaver, Barton and Potter (Figure 1c). These are separated
129 by several gulfs, between 5 and 9 km in width. The peninsulas have a rough topography,
130 peaking at elevations between 120 and 290 m asl. The island has a mild maritime climate, the
131 mean annual temperature at the Bellingshausen Station (Fildes Peninsula) being -2.3 °C (1968-
132 2009, Fernandoy et al., 2012). Precipitation is delivered to the island mainly from eastward

133 moving cyclones within the southern westerlies wind belt (Braun & Hock, 2004). The moisture
 134 source is restricted to the Southern Pacific Ocean and the Amundsen and Bellingshausen seas,
 135 generally between 60 °S and 65 °S (Fernandoy et al., 2012), with a limited contribution from
 136 more northwesterly (including South America) sources. Consequently, a precipitation gradient is
 137 developed from the westernmost peninsula (Fildes) towards the farthest eastern one (Potter),
 138 across Weaver and Barton Peninsulas (Figure 1c). Precipitation falls as snow between April and
 139 November, and as rain and snow, between December and March. Positive temperatures,
 140 gradually melt the snow layer and permafrost beginning in December, the resulting water feeding
 141 streams, lakes and wet, marsh-like areas. Weather observations at King Sejong Station (Barton
 142 peninsula) since 2018 show a reduced amplitude of air temperature variations (between -20.2 °C
 143 and 9.7 °C) and annual precipitation of 363 mm (Kim et al., 2020). This value is low considering
 144 the position of the island, but it might reflect the rain-shadow effect, as Barton peninsula is
 145 shielded from the westerly and north-westerly winds by the Fildes and Weaver peninsulas and
 146 the KGI ice Cap (Figure 1), with important implications for the distribution of stable isotopes in
 147 water (see below).



148
 149 **Figure 1.** Location of the water sampling sites. A) Location of King George Island. B) Map of
 150 King George Island with the location of the investigated peninsulas. C) Sampling locations in
 151 Fildes, Weaver, Barton and Potter Peninsulas.

152 2.2 Sample collection and analysis

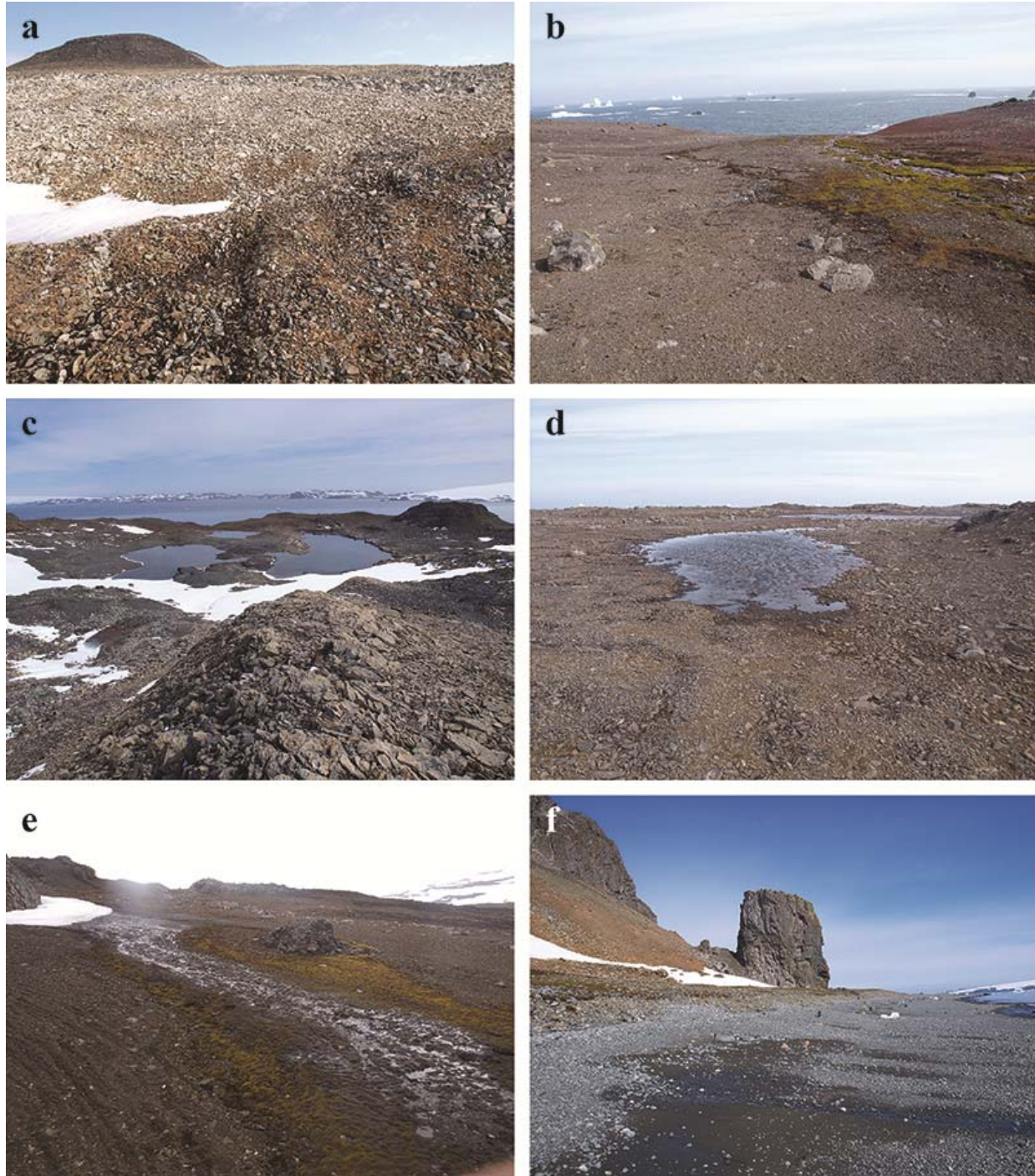
153 We have collected 97 samples of glacier ice, permafrost, snow from the previous winter,
 154 recently falling precipitation, snowmelt, lake, river and groundwater, on the Fildes, Weaver,
 155 Barton and Potter peninsulas (Figure 1c) at the end of melt season in late February 2016. Glacier

156 ice was sampled from above the melting base of the Fourcade Glacier, in Potter Cove (between
157 Barton and Potter peninsulas). Permafrost samples (Figure 2a) were collected around Baekje Hill
158 on Barton Peninsula (200.2 m above sea level), by digging several pits down to the rock/ice
159 interface and mixing together 12 distinctive samples from the permafrost layer. Precipitation
160 samples were collected at King Sejong Station (Barton Peninsula) on February 20, 2016,
161 following a snowstorm. Snow from the previous winter, snowmelt, ground, lake and river water
162 was collected on all peninsulas (between 0 and 200 m above sea level), except Potter Peninsula,
163 where only lake water was sampled (the collection campaign was scheduled after a heavy storm,
164 when all surface waters were mixed with fresh snow). Lake and river water was sampled at 10-
165 50 cm depth below the surface, from ice- and snow-free sectors of the water bodies (Figures 2b
166 and 2c). On Fildes Peninsula, we have also collected lake water samples from three shallow (0.2
167 m) lakes (Figure 2d), during a period of warm, dry and windy weather. Snowmelt was sampled
168 from below melting patches of snow (Figure 2e) and groundwater from water seeping out of
169 ground (Figure 2f). In order to distinguish between permafrost melt and “pure” meltwater, pits
170 were excavated in the rock/soil above the groundwater seepage points and only locations where
171 no direct permafrost input was observed were sampled. Further, snow pits were excavated an the
172 entire now column above the 2014-2015 and 2015-2106 transitional surface was recovered,
173 melted at room temperature and subsequently a 22-ml aliquot was collected for stable isotope
174 analyses. During our field campaign (end of summer), most of the ground was snow-free, and,
175 with few exceptions in Barton and Potter Peninsulas, all lakes were ice-free. All samples were
176 collected in Parafilm[®]-sealed 22 ml HDPE scintillation vials and stored at 4 °C before analyses
177 (in fridge and cooling bags during transport).

178 Stable isotope analyses were performed using a Picarro L2130-*i* CRDS analyzer coupled
179 to a High Precision Vaporizer Module at the Stable Isotope Laboratory, Ștefan cel Mare
180 University (Suceava, Romania). Prior to analysis, samples were filtered using 0.45 μm nylon
181 microfilters. To avoid memory effects, each sample was manually injected at least nine times,
182 and when the standard deviation of the last four injections dropped below 0.03 for δ¹⁸O and 0.3
183 for δ²H respectively, the average of these injections was used as the δ value of the sample. The
184 raw δ value were normalized on the SMOW-SLAP scale using two internal standards calibrated
185 against the VSMOW2 and SLAP2 standards provided by the IAEA. A third standard was used to
186 check the long-term stability of the analyzer. The stable isotope composition of oxygen and
187 hydrogen are reported in the standard δ notation, with precision better than 0.16 ‰ for δ¹⁸O and
188 0.7 ‰ for δ²H (based on repeated measurements of an internal standard), respectively.
189 No precipitation sampling was active during the visits; as such, data for the stable isotope
190 composition in precipitation was obtained from Fernandoy et al. (2012). The samples were
191 collected at the Frei (Barton Peninsula, King George Island) and O’Higgins (Isabel Riquelme
192 Islet, 140 km south of KGI) Chilean Stations between January 2008 and March 2009.

193 **3 Results and discussions**

194 The results of the analysis of water samples from the KGI are presented in Table 1, as
195 average values for the different types of water sampled (lake, river, melt water, groundwater,
196 snow, glacier ice and permafrost), separately for the four peninsulas. In order to better
197 characterize the dataset, we have calculated the mean, maximum, minimum and the amplitude,
198 for both δ¹⁸O and δ²H. On a δ¹⁸O-δ²H diagram (Figure 3), the values plot along the LMWL,
199 defined by Fernandoy et al. (2012) for the O’Higgins station as δ²H = 7.84*δ¹⁸O + 1.2 (black
200 dots in Figure 3).



201

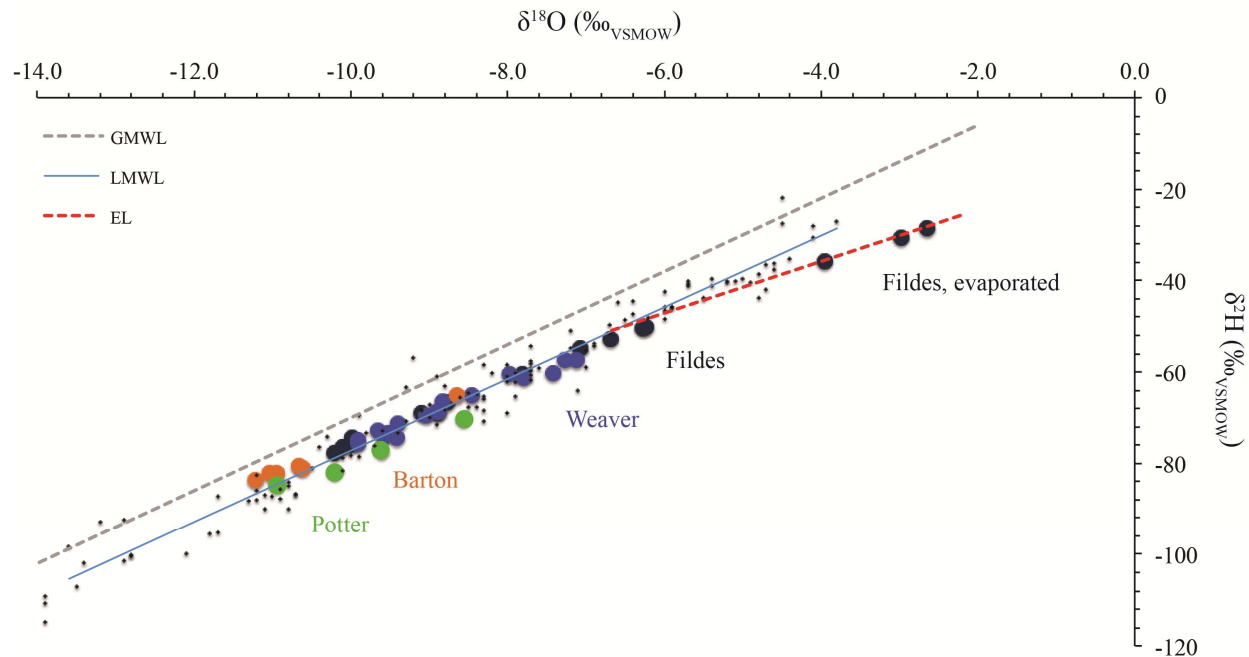
202

203

204

205

Figure 2. General overview of the types of sampling locations: a – site of permafrost sampling, Barton Peninsula, b – river on Fildes Peninsula, c – lakes in Weaver Peninsula, d – evaporatively enriched lake, Fildes Peninsula, e – snowmelt, Fildes Peninsula, f – groundwater seepage, Weaver Peninsula. All photos by Aurel Perşoiu.



206

Figure 3. Stable isotope composition of lake waters in King George Island, shown against the Local (Fernandoy et al., 2012, black dots) and Global Meteoric Water Lines.

207

208

209

210

211

212

213

214

215

216

217

218

219

220

221

222

223

224

225

226

227

228

229

230

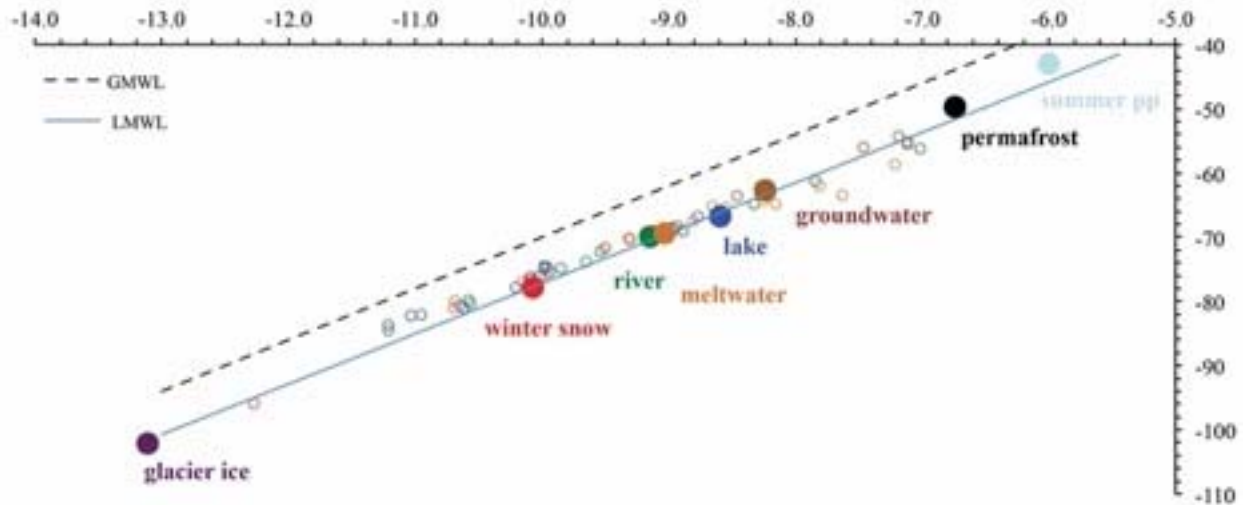
231

232

233

234

Samples from permafrost and groundwater have the highest δ values (Figure 4). The high values of the single permafrost sample might reflect its origin in the partial freezing of infiltration water. Freezing of water is accompanied by strong kinetic fractionation (Jouzel and Souchez, 1982; Perçoiu et al. 2011) and the resulting ice is enriched in heavy isotopes (^{18}O and ^2H) leading to higher than in water δ values. Interestingly, the δ values of groundwater from Barton Peninsula (average values of -7.7‰ for $\delta^{18}\text{O}$ and -58‰ for $\delta^2\text{H}$, respectively) are higher than those found by Kim et al. (2020) for groundwater samples collected in January 2018 (average values of -11.5‰ for $\delta^{18}\text{O}$ and -87‰ for $\delta^2\text{H}$, respectively). Similarly, average δ values of meltwater, snow and lake water in Barton Peninsula (Table 1) at the end of the melt season (February 2016) were higher than in either January 2014 (Lee et al., 2020) or January 2018 (Kim et al., 2020) during the early-to-mid melt season. These differences possibly suggest that during the melt season, fresh snow from the previous winter contributes a larger proportion of water to both lakes and groundwater, and as melting progresses, sources enriched in ^{18}O and ^2H become progressively important in the overall mass (and isotope) balance of surface waters. Several studies (Taylor et al., 2001; Lee et al., 2020 and references therein) have shown a continuous increase of $\delta^{18}\text{O}$ and $\delta^2\text{H}$ in a melting snowpack as a result of isotopic exchange and enrichment in heavy isotopic species as percolating water refreezes inside the snowpack. Thus, we suggest a potential shift in the δ values of surface waters in the region, shift that could be the result of 1) changes in the δ values of source waters (snowpack) and rainfall and/or 2) changes in the relative contribution of different reservoirs to the overall mass balance of surface waters, with meltwater from fresh snow dominating in the early months of summer and diagenetically modified snow and permafrost becoming dominant towards the end of the melt season.



235

236 **Figure 4.** Average $\delta^{18}\text{O}$ and $\delta^2\text{H}$ values in the water bodies in King George Island.

237

238 Lake, river and melt water δ values have a clear decreasing tendency from west (Fildes)
 239 to east (Potter); seen in both mean and maximum values, as well as amplitude, but not so evident
 240 in the minimum values (Table 1). The maximum amplitude of the δ values is seen in lake waters
 241 (up to 4 ‰ for $\delta^{18}\text{O}$ and 23 ‰ for $\delta^2\text{H}$), with groundwaters being more uniform between the
 242 different peninsulas. The deuterium excess (d-excess, defined as $d = \delta^2\text{H} - 8 * \delta^{18}\text{O}$, Dansgaard,
 243 1964) values of all water bodies are low (between -7.4 and 6.1 ‰), suggesting post-depositional
 244 processes are affecting all types of surface waters. The low d-excess values in surface liquid
 245 waters (lakes, rivers and snowmelt) are likely the result of kinetic fractionation of O and H stable
 246 isotopes during evaporation (Craig & Gordon, 1965; Gonfiantini et al., 2018). Strong winds also
 247 very likely resulted in the sublimation and kinetic fractionation of the snowpack, melting having
 248 a reduced effect on the stable isotope composition of snow, due to the very low diffusion
 249 coefficient ($10\text{-}11 \text{ cm}^2 \text{ s}^{-1}$) of the water molecules in ice (Posey & Smith, 1957). However,
 250 isotopic exchange between ice and liquid water (from surface melt) as the later is percolating
 251 through the snowpack could lead to a lower slope of $\delta^{18}\text{O}$ - $\delta^2\text{H}$ line (Zhou et al., 2008; Lee et al.,
 252 2010a, 2010b) and thus further influence the d-excess values of river and lake waters. The
 253 combination of evaporative loss, isotopic exchange between percolating water and snowpack and
 254 strong kinetic fractionation during partial freezing of water followed by melting of the resulting
 255 ice which has low d-excess could thus result in the overall low d-excess values recorded by the
 256 different water bodies in KGI.

257 The $\delta^{18}\text{O}$ and $\delta^2\text{H}$ values of lake waters in KGI were plotted on a $\delta^2\text{H}$ - $\delta^{18}\text{O}$ diagram
 258 against the LMWL and GMWL (Figure 3), and their main characteristics (maximum, minimum,
 259 mean and amplitude values) are shown in Table 1. The three samples collected from shallow
 260 lakes (Figure 2d) have the highest δ values and the lowest d-excess values. They plot on an
 261 “evaporative line” (EL), defined by the equation $\delta^2\text{H} = 5.44 * \delta^{18}\text{O} - 14.35$. Evaporation of surface
 262 waters (Gat, 1981; 2008; Gibson et al., 2005; 2016) results in the enrichment of the remaining
 263 water in the heavy isotopes of O and H, due to lower diffusion rate of the H_2^{18}O and $^2\text{H}^1\text{H}^{16}\text{O}$
 264 isotopologues, compared to $^1\text{H}_2^{16}\text{O}$. The enrichment is proportional to the evaporation rate,

265 which in turn is controlled by relative humidity, temperature and salinity (Gonfiantini, 1986).
266 The ensuing fractionation (a sum of equilibrium and kinetic fractionation, Craig & Gordon,
267 1965; Gonfiantini et al., 2018) results in a slope lower than the LMWL for the line defined by the
268 samples from the residual water (the EL). These three samples whose stable isotope composition
269 reflects evaporative processes (Figure 3), were collected during a period of strong winds that
270 lead to the quick removal of the evaporated water molecules enriched in the light isotopes from
271 the boundary layer and thus minimization of equilibrium and dominance of kinetic fractionation
272 – resulting in the residual water being enriched in heavy isotopologues and alignment along the
273 EL line shown in figure 3. Water from large lakes adjacent to the shallow ones plot at the
274 intersection of the LMWL and the EL, this intersection points likely indicating the stable isotope
275 composition of the shallow lakes' water before evaporation.

276 A clear west to east trend (with increasing distance from the Drake Passage) of δ values
277 in lake waters is evident, with samples from Fildes Peninsula having the highest values, and
278 those from Barton, the lowest. Samples from Potter do not fit in this trend, the δ values being
279 slightly higher than those in Barton, although the peninsula is located further east. Possibly, this
280 difference (although minor) is due to the higher elevation of the sampled lakes in Barton
281 (between 5 and 270 m asl) compared to Potter (~20-60 m asl). Moisture delivered to KGI is
282 originating in the Drake Passage (Fernandoy et al, 2012), west of Barton, so that this W-E trend
283 of decreasing $^{18}\text{O}/^{16}\text{O}$ and $^2\text{H}/^1\text{H}$ ratios is consistent with Rayleigh fractionation processes
284 (Dansgaard, 1964) along a rainout path from the Fildes through Weaver and Barton peninsulas
285 (Figure 3). The W-E trend of lower δ values seen in the stable isotope composition of lake water
286 is mirrored by values in surface (snowmelt and river) waters but not in groundwaters (Table 1),
287 suggesting origin from the same parent source. However, the low number of river and snowmelt
288 samples calls for caution in interpreting this trend in a way similar to that seen in lakes water.

289 We interpret the low d-excess values of surface waters as a result of evaporative (and
290 sublimation in the case of snow) processes affecting all surface water after deposition, resulting
291 in subsequent enrichment in the heavy isotopes of O and H (and associated decrease in d-excess
292 – Table 1). Studies in the Alps (Moser & Stichler, 1975), Antarctica (Satake & Kavada, 1997)
293 and the Andes (Stichler et al., 2001) have shown that sublimation results in enrichment in ^{18}O
294 and ^2H in the remaining snow. Partial melting of this snow and subsequent alimentation of river
295 and lake waters would thus result in the high $\delta^{18}\text{O}$ and $\delta^2\text{H}$ values in surface water samples in
296 KGI.

297 Figure 4 shows the $\delta^{18}\text{O}$ and $\delta^2\text{H}$ values of the different water bodies, allowing for a clear
298 separation of the various water bodies based on their stable isotope values. The stable isotope
299 composition of water in lakes and streams is mainly controlled by that of winter precipitation.
300 Melting of winter snow in summer is the principal source of water for rivers and lakes, with
301 additional input from ^{18}O - (and ^2H -) depleted water (-7.7 through -9.8 ‰ for $\delta^{18}\text{O}$) from
302 degrading permafrost (-6.7 ‰ for $\delta^{18}\text{O}$). Further, following melting of snow, all resulting waters
303 are subjected to strong, wind-driven evaporation, as also indicated by the very low d-excess
304 values (Table 1). Winds are a constant feature of KGI, blowing constantly from a W and SW
305 direction, and thus the continuous evaporation of surface waters results in high $\delta^{18}\text{O}$ and $\delta^2\text{H}$ and
306 low d-excess values.

307 No clear relationship between the stable isotope composition of lake water with altitude
308 has been found, potentially due to the low (less than 300 m) maximum height of the “hills”, thus
309 potentially reducing the ‘altitude-effect’ of the stable isotope composition of precipitation.
310 Nevertheless, the lowest values were found in Barton Peninsula, which has the highest

311 topography of the four investigated areas. While altitude would have played a negligible role, we
312 suggest that sheltering from wind of the lakes (due to the more rugged topography, compared to
313 the other peninsulas) was likely the cause of the low δ values. High d-excess values in lakes from
314 Barton compared with those in the Fildes, Weaver and Potter peninsulas, suggest a lower degree
315 of evaporative fractionation, supporting our inference.

316 **4 Conclusions**

317 The results of stable isotope analyses in water from King George Island indicate 1) a clear
318 separation of the various water bodies in terms of stable isotope composition, likely triggered by
319 the variable contribution of different sources to the final mass (and stable isotope) budget and 2)
320 a general tendency towards lower $\delta^{18}\text{O}$ (and $\delta^2\text{H}$) values with increased distance from the
321 Bellingshausen Sea.

322 KGI is home to the largest concentration of research stations and a permanent settlement
323 in Antarctica, as well as for a wide selection of animal and vegetation life. The results allow for
324 the establishment of a baseline against which ongoing and future alterations of the hydrological
325 cycle could be analyzed, and a better management of the water resources for human and natural
326 usage. Further, our data offers a first step towards potential future studies aiming to quantify the
327 link(s) between climatic conditions and stable isotopes in lake sediments, a necessary tool for
328 future reconstructions of past climate conditions.

329 **Acknowledgments**

330 All stable isotope data that led to this study will be made available in data repositories.
331 The National Institute of Research and Development for Biological Sciences (Bucharest,
332 Romania) and the Korean Polar Institute (KOPRI) financially supported fieldwork in King
333 George Island. AP was further supported by Project IP-SP TofZ during writing of the
334 manuscript. F. Fernandoy provided stable isotope data for precipitation collected at Frey and
335 O'Higgins stations. We thank the personnel at King Sejong (South Korea), Belingshaussen
336 (Russia, especially Bulat Mavlyudov) and Carlini (Argentina) stations in King George Island for
337 logistic supports, discussions and hot *herba mate* when most needed. The authors declare no
338 conflicts of interest.

339 **References**

- 340 Ala-aho, P., Soulsby, C., Pokrovsky, O. S., Kirpotin, S. N., Karlsson, J., Serikova, S., et al.
 341 (2018). Using stable isotopes to assess surface water source dynamics and hydrological
 342 connectivity in a high-latitude wetland and permafrost influenced landscape. *Journal of*
 343 *Hydrology*, 556, 279–293. <https://doi.org/10.1016/j.jhydrol.2017.11.024>
- 344 Amesbury, M. J., T. P. Roland, J. Royles, D. A. Hodgson, P. Convey, H. Griffiths, and D. J.
 345 Charman (2017). Widespread Biological Response to Rapid Warming on the Antarctic
 346 Peninsula, *Current Biology*, 27(11), 1616-1622.
 347 <https://doi.org/10.1016/j.cub.2017.04.034>
- 348 Aracena, C., H. E. González, J. Garcés-Vargas, C. B. Lange, S. Pantoja, F. Muñoz, E. Teca, and
 349 E. Tejos (2018). Influence of summer conditions on surface water properties and
 350 phytoplankton productivity in embayments of the South Shetland Islands. *Polar Biology*,
 351 41(10), 2135-2155. <https://doi.org/10.1007/s00300-018-2338-x>
- 352 Arnoux, M., Gibert-Brunet, E., Barbecot, F., Guillon, S., Gibson, J. J., & Noret, A. (2017).
 353 Interactions between groundwater and seasonally ice-covered lakes: Using water stable
 354 isotopes and radon-222 multilayer mass balance models. *Hydrological Processes*, 31(14),
 355 2566–2581. <https://doi.org/10.1002/hyp.11206>
- 356 Barnett, T.P., Adam, J.C., Lettenmaier, D.P. (2005). Potential impacts of a warming climate on
 357 water availability in snow-dominated regions. *Nature*, 438, 303–309.
 358 <https://doi.org/10.1038/nature04141>
- 359 Braun, M., & Hock, R. (2004). Spatially distributed surface energy balance and ablation
 360 modelling on the ice cap of King George Island (Antarctica). *Global and Planetary*
 361 *Change*, 42(1), 45–58. <https://doi.org/10.1016/j.gloplacha.2003.11.010>
- 362 Bowen, G. J. (2010). Isoscapes: spatial pattern in isotopic biogeochemistry. *Annual Review of*
 363 *Earth and Planetary Sciences* 38 (1), 161–187. [https://doi.org/10.1146/annurev-earth-](https://doi.org/10.1146/annurev-earth-040809-152429)
 364 [040809-152429](https://doi.org/10.1146/annurev-earth-040809-152429)
- 365 Craig, H. (1961). Isotope variations in meteoric waters. *Science*, 133, 1702–1703.
 366 <https://doi.org/10.1126/science.133.3465.1702>
- 367 Craig, H., & Gordon, L.I. (1965). Deuterium and oxygen 18 variations in the ocean and the
 368 marine atmosphere. In E. Tongiorgi (Ed.), *Stable Isotopes in Oceanographic Studies and*
 369 *Paleotemperatures* (pp. 9-130). Pisa: Consiglio Nazionale delle Ricerche, Laboratorio di
 370 Geologia Nucleare
- 371 Dansgaard, W. (1964). Stable isotopes in precipitation. *Tellus*, 16(4), 436–468.
 372 <https://doi.org/10.1111/j.2153-3490.1964.tb00181.x>
- 373 Delavau, C., Sun, C., Stadnyk, T., McDonald, J., Birks, J., & Welker, J. M. (2015). Time series
 374 modeling of precipitation isotopes ($\delta^{18}\text{O}$) across Canada and the northern United States.
 375 *Water Resources Research*, 51(2), 1284–1299. <https://doi.org/10.1002/2014WR015687>
- 376 Falk, U. & Sala, H. (2015) Winter melt conditions of the inland ice cap on King George Island,
 377 Antarctic Peninsula, *Erdkunde*, 69(4), 341-363.
 378 <https://doi.org/10.3112/erdkunde.2015.04.04>
- 379 Falk, U., A. Silva-Busso, and P. Pölcher (2018), A simplified method to estimate the run-off in
 380 Periglacial Creeks: a case study of King George Islands, Antarctic Peninsula.
 381 *Philosophical Transactions of the Royal Society A: Mathematical, Physical and*
 382 *Engineering Sciences*, 376(2122), 20170166. <https://doi.org/10.1098/rsta.2017.0166>
- 383 Hernández, A. C., Bastias, J., Matus, D., & Mahaney, W. C. (2018). Provenance, transport and
 384 diagenesis of sediment in polar areas: a case study in Profound Lake, King George Island,

- 385 Antarctica. *Polar Research*, 37, 1490619.
386 <https://doi.org/10.1080/17518369.2018.1490619>
- 387 Fernandoy, F., Meyer, H., & Tonelli, M. (2012). Stable water isotopes of precipitation and firn
388 cores from the northern Antarctic Peninsula region as a proxy for climate reconstruction.
389 *The Cryosphere*, 6(2), 313–330. <https://doi.org/10.5194/tc-6-313-2012>
- 390 Gat, J. R. (1981). Lakes. In J. R. Gat & R. Gonfiantini (Eds.) *Stable Isotope Hydrology –*
391 *Deuterium and Oxygen-18 in the Water Cycle* (Technical Report Series No. 210, pp.
392 203–221), Vienna: International Atomic Energy Agency.
- 393 Gat, J. R. (2008). The isotopic composition of evaporating waters – review of the historical
394 evolution leading up to the Craig–Gordon model. *Isotopes in Environmental and Health*
395 *Studies*, 44 (1), 5–9. <https://doi.org/10.1080/10256010801887067>
- 396 Gibson, J. J., Edwards, T. W. D., Birks, S. J., St Amour, N. A., Buhay, W. M., McEachern, P., et
397 al. (2005). Progress in isotope tracer hydrology in Canada. *Hydrological Processes*,
398 19(1), 303–327. <https://doi.org/10.1002/hyp.5766>

- 399 Gibson, J. J., Birks, S. J., Yi, Y., & Vitt, D. H. (2015). Runoff to boreal lakes linked to land
400 cover, watershed morphology and permafrost thaw: a 9-year isotope mass balance
401 assessment. *Hydrological Processes*, 29(18), 3848–3861.
402 <https://doi.org/10.1002/hyp.10502>
- 403 Gibson, J.J., Birks, S.J., & Yi, Y. (2016). Stable isotope mass balance of lakes: a contemporary
404 perspective. *Quaternary Science Reviews*, 131, 316-328.
405 <https://doi.org/10.1016/j.quascirev.2015.04.013>
- 406 Gómez, M., M. Concepción Ausín, and M. Carmen Domínguez (2017), Seasonal copula models
407 for the analysis of glacier discharge at King George Island, Antarctica. *Stochastic*
408 *Environmental Research and Risk Assessment*, 31(5), 1107-1121.
409 <https://doi.org/10.1007/s00477-016-1217-7>
- 410 Gonfiantini, R. (1986). Environmental isotopes in lake studies. In P. Fritz & J. C. Fontes (Eds.)
411 *Handbook of Environmental Isotope Geochemistry* (Vol. 3., pp. 113–168), New York:
412 Elsevier
- 413 Gonfiantini, R., Wassenaar, L. I., Araguas-Araguas, L., & Aggarwal, P. K. (2018). A unified
414 Craig-Gordon isotope model of stable hydrogen and oxygen isotope fractionation during
415 fresh or saltwater evaporation. *Geochimica et Cosmochimica Acta*, 235, 224–236.
416 <https://doi.org/10.1016/j.gca.2018.05.020>
- 417 Hass, H. C., G. Kuhn, P. Monien, H. J. Brumsack, and M. Forwick (2010). Climate fluctuations
418 during the past two millennia as recorded in sediments from Maxwell Bay, South
419 Shetland Islands, West Antarctica. *Geological Society, London, Special Publications*,
420 344(1), 243. <https://doi.org/10.1144/SP344.17>
- 421 Headland, R. K. (1984). *The Island of South Georgia*. Cambridge: Cambridge University Press.
- 422 Jespersen, R. G., Leffler, A. J., Oberbauer, S. F., & Welker, J. M. (2018). Arctic plant
423 ecophysiology and water source utilization in response to altered snow: isotopic ($\delta^{18}\text{O}$
424 and $\delta^2\text{H}$) evidence for meltwater subsidies to deciduous shrubs. *Oecologia*, 187(4), 1009–
425 1023. <https://doi.org/10.1007/s00442-018-4196-1>
- 426 Jouzel, J. & Souchez, R. A. (1982). Melting refreezing at the glacier sole and the isotopic
427 composition of the ice. *Journal of Glaciology*, 28, 35-42
- 428 Mäusbacher, R., Muller, J., Munnich, M., & Schmidt, R. (1989). Evolution of postglacial
429 sedimentation in Antarctic lakes (King George Island). *Zeitschrift für Geomorphologie*,
430 33(2), 219-234. <https://doi.org/10.1127/zfg/33/1989/219>
- 431 Meredith, M. P., U. Falk, A. V. Bers, A. Mackensen, I. R. Schloss, E. Ruiz Barlett, K. Jerosch,
432 A. Silva Busso, and D. Abele (2018). Anatomy of a glacial meltwater discharge event in
433 an Antarctic cove. *Philosophical Transactions of the Royal Society A: Mathematical,*
434 *Physical and Engineering Sciences*, 376(2122), 20170163.
435 <https://doi.org/10.1098/rsta.2017.0163>
- 436 Moser, H. & Stichler, W. (1975). Deuterium and oxygen-18 contents as an index of the
437 properties of snow covers. IAHS Publication 114 (Symposium at Grindelwald 1974 –
438 Snow Mechanics), 122–135.
- 439 Noon, P. E., Leng, M., Arrowsmith, C., Edworthy, M., & Strachan, R. (2002). Seasonal
440 observations of stable isotope variations in a valley catchment, Signy Island, South
441 Orkney Islands. *Antarctic Science*, 14(4), 333–342.
442 <https://doi.org/10.1017/S0954102002000159>

- 443 Noon, P. E., Leng, M. J., & Jones, V. J. (2003). Oxygen-isotope ($\delta^{18}\text{O}$) evidence of Holocene
444 hydrological changes at Signy Island, maritime Antarctica. *The Holocene*, 13(2), 251-
445 263. <https://doi.org/10.1191/0959683603hl611rp>
- 446 Pachauri, R. K., Allen, M. R., Barros, V. R., Broome, J., Cramer, W., Christ, R. et al. (2014).
447 Climate Change 2014: Synthesis Report. Contribution of Working Groups I, II and III to
448 the Fifth Assessment Report of the Intergovernmental Panel on Climate Change [Core
449 Writing Team, R.K. Pachauri and L.A. Meyer (eds.)]. IPCC, Geneva, Switzerland, 151
450 pp.
- 451 Perşoiu, A., Onac, B. P., Wynn, J., Bojar, A.-V., & Holmgren, K. (2011) Stable isotopes
452 behavior during cave ice formation by water freezing in Scărișoara Ice Cave. *Journal of*
453 *Geophysical Research - Atmospheres*, 116, D02111.
454 <https://doi.org/10.1029/2010JD014477>
- 455 Peterson, B. J., Holmes, R. M., McClelland, J. W., Vörösmarty, C. J., Lammers, R. B.,
456 Shiklomanov, A. I., et al. (2002). Increasing river discharge to the Arctic Ocean. *Science*,
457 298, 2171–2173. <https://doi.org/10.1126/science.1077445>
- 458 Posey, J. C., & Smith, H. A. (1957). The equilibrium distribution of light and heavy waters in a
459 freezing mixture. *Journal of the American Chemical Society*, 79, 555–557.
460 <https://doi.org/10.1021/ja01560a015>
- 461 Quinton, W., Hayashi, M., & Chasmer, L. (2011). Permafrost-thaw-induced land-cover change
462 in the Canadian subarctic: implications for water resources. *Hydrological Processes*, 25,
463 152–158. <https://doi.org/10.1002/hyp.7894>
- 464 Rückamp, M., M. Braun, S. Suckro, and N. Blindow (2011). Observed glacial changes on the
465 King George Island ice cap, Antarctica, in the last decade. *Global and Planetary Change*,
466 79(1), 99-109. <https://doi.org/10.1016/j.gloplacha.2011.06.009>
- 467 Satake, H. & Kawada, K. (1997). The quantitative evaluation of sublimation and the estimation
468 of original hydrogen and oxygen isotope ratios of a firn core at East Queen Maud Land,
469 Antarctica. *Bulletin of Glacier Research*, 15, 93–97.
- 470 Szilo, J., and R. J. Bialik (2017). Bedload transport in two creeks at the ice-free area of the
471 Baranowski Glacier, King George Island, West Antarctica. *Polish Polar Research*, 38
472 (No 1), 21-39
- 473 Stichler, W., Schotterer, U., Fröhlich, K., Ginot, P., Kull, C., Gäggeler, H., et al. (2001).
474 Influence of sublimation on stable isotope records recovered from high-altitude glaciers
475 in the tropical Andes. *Journal of Geophysical Research: Atmospheres*, 106(D19), 22613–
476 22620. <https://doi.org/10.1029/2001JD900179>
- 477 Stowe, M., Harris, C., Hedding, D., Eckardt, F., & Nel, W. (2018). Hydrogen and oxygen isotope
478 composition of precipitation and stream water on sub-Antarctic Marion Island. *Antarctic*
479 *Science*, 30(2), 83–92. <https://doi.org/10.1017/S0954102017000475>
- 480 Taylor, S., Feng, X., Kirchner, J. W., Osterhuber, R., Klaue, B. & Renshaw, C. E. (2001).
481 Isotopic evolution of a seasonal snowpack and its melt. *Water Resources Research* 37(3),
482 759–769. <https://doi.org/10.1029/2000WR900341>
- 483 Tetzlaff, D., Piovano, T., Ala-Aho, P., Smith, A., Carey, S. K., Marsh, P., Wookey, P. A., Street,
484 L. E. & Soulsby, C. (2018). Using stable isotopes to estimate travel times in a data-sparse
485 Arctic catchment: Challenges and possible solutions. *Hydrological Processes*, 32(12),
486 1936–1952. <https://doi.org/10.1002/hyp.13146>

- 487 Turner, J., Lu, H., White, I., King, J. C., Phillips, T., Hosking, J. S., et al. (2016). Absence of 21st
488 century warming on Antarctic Peninsula consistent with natural variability. *Nature*, 535,
489 411–415. <https://doi.org/10.1038/nature18645>
- 490 Turner, J., Colwell, S. R., Marshall, G. J., Lachlan-Cope, T. A., Carleton, A. M., Jones, P. D., et
491 al. (2005). Antarctic climate change during the last 50 years. *International Journal of*
492 *Climatology*, 25, 279–294 (2005). <https://doi.org/10.1002/joc.1130>
- 493 Vaughan, D. G., G. J. Marshall, W. M. Connolley, C. Parkinson, R. Mulvaney, D. A. Hodgson,
494 J. C. King, C. J. Pudsey, and J. Turner (2003). Recent Rapid Regional Climate Warming
495 on the Antarctic Peninsula. *Climatic Change*, 60(3), 243-274. [https://doi.org/](https://doi.org/10.1023/A:1026021217991)
496 [10.1023/A:1026021217991](https://doi.org/10.1023/A:1026021217991)
- 497 Vieira, G., et al. (2010). Thermal state of permafrost and active-layer monitoring in the antarctic:
498 Advances during the international polar year 2007–2009. *Permafrost and Periglacial*
499 *Processes*, 21(2), 182-197. <https://doi.org/10.1002/ppp.685>
- 500 Walvoord, M. A., & Kurylyk, B. L. (2016). Hydrologic impacts of thawing permafrost – a
501 review. *Vadose Zone Journal*, 15(6), 1–20. <https://doi.org/10.2136/vzj2016.01.0010>
- 502 Wand, U., Hermichen, W.-D., Brüggemann, E., Zierath, R., & Klokov, V. D. (2011). Stable
503 isotope and hydrogeochemical studies of Beaver Lake and Radok Lake, MacRobertson
504 Land, East Antarctica. *Isotopes in Environmental and Health Studies*, 47(4), 407–414.
505 <https://doi.org/10.1080/10256016.2011.630465>
- 506 Wassenaar, L. I., Athanasopoulos, P., & Hendry, M. J. (2011). Isotope hydrology of
507 precipitation, surface and ground waters in the Okanagan Valley, British Columbia,
508 Canada. *Journal of Hydrology*, 411(1–2), 37–48.
509 <https://doi.org/10.1016/j.jhydrol.2011.09.032>
- 510 Welp, L., Randerson, J., Finlay, J., Davydov, S., Zimova, G., Davydova, A., et al. (2005). A
511 high-resolution time series of oxygen isotopes from the Kolyma River: implications for
512 the seasonal dynamics of discharge and basin-scale water use. *Geophysical Research*
513 *Letters*, 32, L14401. <https://doi.org/10.1029/2005GL022857>
- 514 Yde, J. C., Knudsen, N. T., Steffensen, J. P., Carrivick, J. L., Hasholt, B., Ingeman-Nielsen, T.,
515 et al. (2016). Stable oxygen isotope variability in two contrasting glacier river catchments
516 in Greenland. *Hydrology and Earth System Science*, 20, 1197–1210.
517 <https://doi.org/10.5194/hess-20-1197-2016>
- 518 Zakharova, E., Kouraev, A., Kolmakova, M., Mognard, N., Zemtsov, V., & Kirpotin, S. (2009).
519 The modern hydrological regime of the northern part of Western Siberia from in situ and
520 satellite observations. *International Journal of Environmental Studies*, 66, 447–463.
521 <https://doi.org/10.1080/00207230902823578>
- 522 Zhou, S., M. Nakawo, S. Hashimoto, & A. Sakai (2008). The effect of refreezing on the isotopic
523 composition of melting snowpack. *Hydrological Processes*, 22(6), 873-882.
524 <https://doi.org/10.1002/hyp.6662>

		$\delta^{18}\text{O}$ (‰ _{VSMOW})				$\delta^2\text{H}$ (‰ _{VSMOW})				d-excess
		Mean	Min	Max	Amplitude	Mean	Min	Max	Amplitude	
Lakes	Fildes (14)	-8.7	-10.2	-6.2	4.0	-67	-78	-50	28	2.7
	Fildes, evaporated (3)	-4.3	-6.3	-2.6	3.7	-38	-51	-29	22	-4.0
	Weaver (17)	-8.8	-9.9	-7.1	2.8	-68	-76	-57	19	2.4
	Barton (5)	-10.9	-11.2	-10.6	0.6	-82	-84	-81	3	5.2
	Potter (4)	-9.8	-10.9	-8.6	2.3	-79	-85	-72	13	0.1
Rivers	Fildes (10)	-8.8	-10.1	-7.0	3.1	-68	-76	-55	21	2.4
	Weaver (3)	-9.0	-9.7	-8.3	1.4	-70	-74	-65	9	2.0
	Barton (3)	-10.8	-11.2	-10.6	0.6	-82	-85	-80	5	4.7
Meltwater	Fildes (14)	-8.5	-10.3	-7.2	3.1	-66	-77	-59	18	2
	Weaver (3)	-9.8	-10.1	-9.5	0.6	-76	-77	-75	2	2
	Barton (7)	-9.8	-10.7	-8.7	2.0	-74	-81	-65	16	4
Groundwater	Fildes (4)	-8.5	-9.5	-7.1	2.4	-65	-72	-55	17	3
	Weaver (1)	-9.0	-	-	-	-69	-	-	-	3
	Barton (3)	-7.7	-8.5	-7.2	1.3	-58	-64	-54	10	4
Snow (3)	Fildes/Weaver/Barton	-10.1	-12.3	-8.6	3.7	-78	-96	-67	29	2.8
Glacier (1)	Potter/Barton	-13.1	-	-	-	-102	-	-	-	3
Permafrost (1)	Barton	-6.7	-50	-	-	-	-	-	-	4
Precipitation (1)	Barton	-6.0	-	-	-	-43	-	-	-	5

525

526

Table 1. Main characteristics of the stable isotope composition of surface waters in King George Island, Antarctica.